Desalination and Water Treatment
www.deswater.com
doi: 10.1080/19443994.2013.848652

52 (2014) 1615–1623
February

Taylor & Francis
Taylor & Francis Group

Catalytic oxidation of high-concentration ammonia in groundwater by a naturally formed co-oxide filter film

Ting-lin Huang*, Xin Cao, Qian Zhang, Zhi-min Su, Na Zheng

School of Environmental and Municipal Engineering, Xi'an University of Architecture and Technology, No. 13, Yanta Road, Xi'an 71055, Shannxi Province, P.R. China
Tel. +86 29 82201038; Fax: +86 29 82201038; email: huangtinglin@xauat.edu.cn

Received 28 November 2012; Accepted 8 September 2013

ABSTRACT

Operation of a sand filter system in treating groundwater produces a high concentration of ammonia (2–2.8 mg L^{-1}), iron (0.9–2 mg L^{-1}) and manganese (1.2–1.7 mg L^{-1}), and on the surfaces of quartz sands, a co-oxide filter film is formed. The removal of ammonia in the filter before and after the treatment of film-coated sands at high temperature and pressure and the transformation of nitrogen in filter bed were studied. The morphology and chemical composition of film-coated sands were studied by SEM and EDS, respectively, and the structure of the film material was characterized by XRD. The specific area and pore properties of quartz sands before and after the formation of the filter film were studied by the BET method. The X-ray photoelectron spectroscopy characterization was introduced to identify the chemsorb sites of dissolved oxygen and ammonia on the film surface. The results show that the film material consisting of iron and manganese oxides was amorphous; both specific area and pore volume of the sands got increased as the film was formed. Removal of ammonia in the filter was a catalytic oxidation process, and 90% of capacity of ammonia treatment was recovered in the 116 h operation after the film-coated sands got treated at high temperature and pressure, which was due to the restoration of the surface structure of the film. The dissolved oxygen was most possibly adsorbed on Mn atoms occurring as Mn_2O_3 and MnO_2, and the Fe atoms occurring as FeO while on the membrane surface, the Mn atoms in states of Mn_2O_3 and MnO, and the Fe atoms in states of Fe_2O_3 and FeO may be the chemsorb sites of ammonia.

Keywords: Ammonia removal; Catalytic oxidation; Chemisorb site; Filter film

1. Introduction

The modern medical theory suggests that the excess ammonia has toxic effects on the central nervous system, especially in developing brain; leads to irreversible damage; causes presentation symptoms such as cognitive impairment, seizures and cerebral palsy [1,2]. Moreover, ammonia can compromise disinfection efficiency, resulting in nitrite formation in distribution systems, and cause the taste and odour problems [3]. According to the standards of drinking water quality of China, the acceptable ammonia concentration in drinking water is generally lower than 0.5 mg L^{-1}.

*Corresponding author.

Presented at the Conference on Water Resources and Urbanization Development, 26–27 September 2012, Tianjin, China

However, in China, nearly 10.6% of groundwater resources got ammonia pollution problem and the situation is still taking a turn for the worse [4].

Some methods such as adsorption, ion exchange [5,6] and bio-treatment [7,8] have been investigated for removal of ammonia from drinking water. The present studies on adsorption methods mostly focus on the properties and the modification of the adsorbent; also the operating conditions were studied and optimized to improve the ion exchange process. The active carbons derived from rice husk are used to adsorb ammonia in aqueous solution [9], and activated carbon-adsorbed NH_4^+-N should be used for fertilizer conservation, especially for nitrogen. Wang et al. have compared the efficiency of ion exchange of several materials for removal of low-concentration ammonia [10], and found that compared with Na-ferrierite, Na-ZSM-5, Na-b and Na-Y, and the K-and H-form mordenite, Na-mordenite was the most efficient cation exchanger, and under certain conditions, the removal of ammonia can reach 79.1%. An electrochemical-ion exchange reactor with a Cu/Zn as cathode and a Ti/IrO_2-Pt as anode and zeolites as ion exchanger was designed by Li et al. [11]. Ammonia can be removed harmlessly without resulting in the second pollution. Most of the studies mentioned above were done under the experimental scale and the costs in modification, regeneration and operation making the application of these studies were limited. The present studies on bio-treatment of ammonia were mostly carried out on pilot-scale or full-scale units or in situ conditions. The operating conditions were investigated to optimize the biological effects; also some operations were carried out to increase the population and the activities of the ammonia-oxidizing microbes. Andersson and Lauent studied the impact of temperature on nitrification in biologically activated carbon filters [12], and found that the removal of ammonia in the filter decreased from 90 to nearly 30%, when the temperature changed from 10 to 4˚C. The simultaneous COD, NH_4^+-N and Mn^{2+} removal from drinking water by a biological aerated filter was studied [13], and the COD load, aeration rate and hydraulic retention time were considered as three operational variables to determine the optimum conditions of operation. The removal of COD, NH_4^+–N and Mn^{2+} in optimum conditions was 95.5, 93.9 and 94.8%, respectively. Biological removal of ammonia, iron and manganese from potable water was studied in a pilot-scale trickling filter [7], and the results show that the mean size of the gravel and, hence, the specific surface area plays a key role in optimal ammonia removal rates. In a full-scale GAC plant, the settlement of ammonia-oxidizing archaea (AOA) and bacteria (AOB) were monitored [14], and the result suggests that AOA may account for most of the ammonia oxidation. The performance of a full-scale groundwater filter with nitrification problems and another filter with complete nitrification and pretreatment by subsurface aeration was monitored over nine months, and by using quantitative real-time polymerase chain reaction (qPCR) targeting the amoA gene of bacteria and archaea and activity measurements of ammonia oxidation, the water and filter sand samples got from systems were regularly evaluated [15]. Results demonstrated that subsurface aeration stimulated the growth of ammonia-oxidizing prokaryotes in the aquifer, and the incomplete nitrification was caused by nutrient limitation. However, the microbes introduced into drinking water treatment may release the organic materials into water and then bring the risks of disinfection by-products which once have been proved to be the kinds of carcinogen [16].

The pollutants as well as the micro-organism settlements of water resources in each study are of diversity. So, the divergences in each theory are inevitable, and it is necessary to study the special mechanism of ammonia removal to meet the requirement for the water treatment in a certain region.

In the present study, the ammonia in iron- and manganese-contained groundwater in the north-west region of Xi'an was treated by a pilot-scale sand filter, and as the plant operation goes on, the sands in the filter were coated by a deep colour filter film consisting of co-oxides of iron and manganese. It was found that the filter film has the catalytic activity on oxidation of ammonia. It is significant to enhance this kind of a catalytic oxidation process, for on the one hand, the dissolved oxygen used in the process as oxidant can be acquired and adjusted by aeration which can be achieved easily and economically, and on the other hand, the ammonia pollutant can be removed only by physical and chemical effects, but not any biological effect, the risks of disinfection by-products can be originally avoided. The research on the mechanism of ammonia catalytic oxidation may be widely used in drinking water supplement as well as other areas of high ammonia water treatment in the future and is necessary and prospective.

2. Materials and methods

2.1. Pilot-scale filter system

The pilot-scale filter system, shown in Fig. 1, consists of four units which are pump system, spray aeration unit, degasser and quartz sand fixed bed filter, respectively.

The raw groundwater was pumped from the well at the depths of 40 m north-west of the city of Xi'an. The water quality and the standard values of drinking water are shown in Table 1.

The filter consists of a 380 cm high Plexiglas tube with the inside diameter of 15 cm, the bed and support layers fixed in it were 180 and 30 cm high and the diameter of sands in each parts are 1–2 mm and 1–2 cm, respectively. In the first two units, the raw water was aerated and the CO_2 dissolved in groundwater was degassed, which increased the DO in the water to nearly 7.2 mg L^{-1}, which was further increased to nearly 7.8 mg L^{-1} when the water fell into the filter. The filtering process was operated under the velocity of 8 m/h, and backwashing process consisted of air backwash, air-water backwash and water backwash. In each step, the intensity of air and water backwash was 13–17 and 3–4 L/s m^2, respectively.

2.2. Analytical methods

All the chemicals were of reagent grade and all solutions were prepared using deionized water. The results were obtained in duplicate tests. The inflow and outflow water samples of the filter system were collected and analysed at regular intervals and the methods used were as follows: the concentrations of iron and manganese were determined by using an atomic absorption spectrophotometer (GBC-Avanta PM); the total nitrogen was determined by alkaline potassium persulfate digestion-UV spectrophotometric method, the concentration of ammonia was spectrophotometrically determined by Nessler reagent method; and nitrites were determined by the method with sulphanilic acid and α-naphthylamine, and nitrates by dimethylphenol [17]. The DO, pH and temperature of the raw water were determined by HACH-HQ30d.

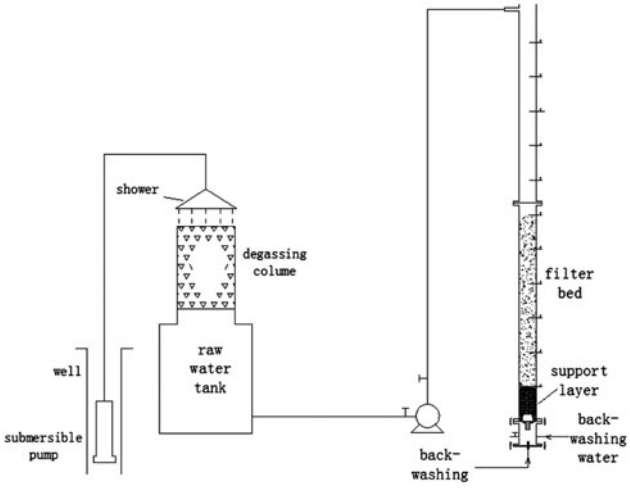

Fig. 1. Schematic representation of the pilot-scale filter system.

Table 1
Quality of raw groundwater and corresponding standard values.

Parameters	Raw water	Standard values
T, ℃	10–20	–
pH	7.5–7.8	6.5–8.5
DO, mg L^{-1}	2.5–3.5	/
NH_4^+-N, mg L^{-1}	2–2.8	0.5
NO_3-N, mg L^{-1}	0	10
NO_2-N, mg L^{-1}	0.001–0.003	1.0
Iron, mg L^{-1}	0.9–2.0	0.3
Manganese, mg L^{-1}	1.2–1.7	0.1

2.3. Characterization of the filter membrane

The co-oxides film coated on the sands was peeled by shear force provided by water shaking at a high speed and an ordinary temperature. The samples were collected and dried in a vacuum desiccator at room temperature. Both film samples and fresh filter sands were characterized by an X-ray diffraction analysis over a range of 15–65° in the steps of 0.2 with Cu Kα radiation.

The samples of sands were immobilized by glutaria aldehyde and the surface elements and morphologies of the samples were served by a scanning electron microscope (JEOL-JSM6360LV and Hitachi S-4800IIFE-SEM in 50 k times amplification) with an X-ray energy spectrum instrument (Thermo Fisher Scientific-Noran System six).

The specific surface and pore size of the fresh and film-coated sands were obtained by using the BET method (Quantachrome-AUTOSORB-1C).

The chemsorb active sites of ammonia and dissolved oxygen on the film were detected by studying the binding energy change before and after the corresponding adsorption. The solution of ammonia was prepared with oxygen-free deionized water, and the concentrations of DO were regulated by nitrogen filling. The cleaned co-oxidize film-coated sands got

chemsorb equilibrium and dried at room temperature in a vacuum tube. The binding energies were measured by X-ray photo electron spectroscopy (Thermo Scientific K-Alpha). A conventional Al K α anode radiation source was used as the excitation source. The binding energies were calibrated by the C 1s binding energy at 284.8 eV. X-ray photoelectron spectroscopy (XPS) data processing and peak fitting were done by using the corresponding software (Avantage).

3. Results and discussion

3.1. Performance of the pilot-scale filter system

To exclude the possible biologic effect in the process of ammonia removal, the sands fixed in the pilot-scale filter coated by the co-oxides film were treated at 120°C and 0.12 Mpa, and then fixed back into the filter. The removal of ammonia before and after the treatment is shown in Fig. 2.

As shown in Fig. 2, treated under high temperature and pressure, the co-oxides film coated on the sands was partly peeled off and made the removal of ammonia decreased obviously from 89.4 to nearly 23.1% at the beginning of the operation. During the period of 68–116 h, the capacity of ammonia removal in the filter recovered obviously from 30.3 to 83.2% and finally was maintained at nearly 80% after 116 h of operation. This may be due to the fact that the coverage of the co-oxide film on the sand surface got restored, and the ammonia catalytic oxidation activity was recovered.

The concentrations of TN, ammonia, nitrite and nitrate, as well as the DO of different depths in the filter bed, were measured after 178 h of operation. The results are shown in Fig. 3. The removal of ammonia and the consumption of dissolved oxygen were calculated and are listed in Table 2.

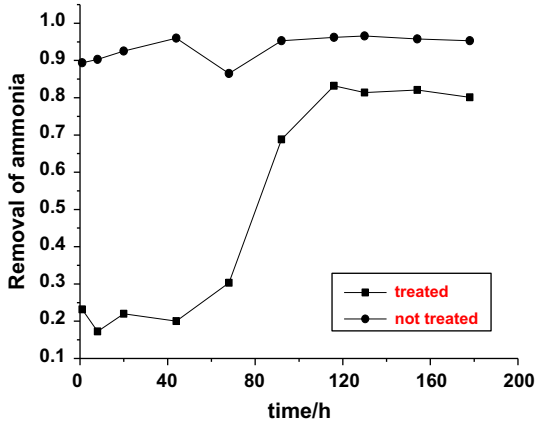

Fig. 2. Removal of ammonia in the sand filter fixed with treated and not treated sands.

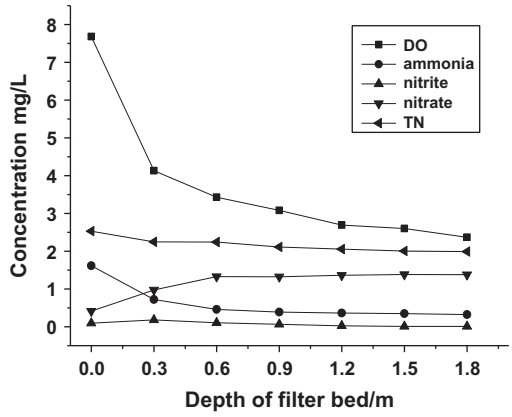

Fig. 3. Concentrations of DO, ammonia, nitrite, nitrate and TN at different depths of the filter bed after 178 h operation.

It is evident from Table 2 that the removal of ammonia can reach nearly 71.7% at the depth range from 0 to 0.6 m correspondingly, and nearly 55.3% of DO in water was consumed. Also, at the same depths as shown in Fig. 3, the concentration of ammonia decreased by 1.17 mg L^{-1} while the nitrite and nitrate increased totally by 1.01 mg L^{-1}, which means that the element of nitrogen is generally in mass balance. The oxidation process mainly happened at the depth of 0.6 m, and as the depth increased, the decreased concentrations of ammonia as well as dissolved oxygen made the oxidation process slow down and the concentrations of each indexes stayed in a relatively stable state. The coordinate changes of these indexes indicate that the ammonia removal is a chemical oxidation process instead of biologic effects [18]. The TN of each depth is higher by nearly 0.35 mg L^{-1} than the sum of ammonia, nitrite and nitrate, which indicates the existence of organic nitrogen.

Table 2
Removal of ammonia and consumption of DO at depths.

Depths, m	DO consumption, %	NH_4^+-N removal, %
0	0	0
0.3	46.2	55.3
0.6	55.3	71.7
0.9	59.9	75.9
1.2	64.9	77.6
1.5	66.1	78.3
1.8	69.1	80.0

3.2. Co-oxide membrane characterization

3.2.1. X-ray diffusion

Both film samples and fresh filter sands were characterized by XRD and results are shown in Fig. 4

As shown in Fig. 4, the fresh sands pattern with the three characteristic peaks at 20.84, 26.52, and 36.50° shows the crystal structure of quartz, while the XRD pattern of the film was irregular and cluttered, and no obvious characteristic peak was identified. It is expected that during the formation of the film, the oxides are generated on the surface of the sands at random and form amorphous structures, which may provide the increased specific area and optimized pore properties [19] for catalytic oxidation of ammonia.

3.2.2. Morphology

The samples of fresh sands, film-coated sands and the film-coated sands treated at high temperature and pressure and operated after 178 h were characterized by SEM; the elements composition was analysed by EDS; and the results are shown in Figs. 5–7.

It can be seen from Fig. 5 that the texture of fresh sand is compact and the surface is full of cracks with the size of 5–10 μm. The quantitative analysis from EDS shows that the atomic ratio of Si to O is close to 2:1, which indicates the quartz constituent.

As shown in Fig. 6, the co-oxide film coats the sands uniformly, and the texture of the film surface is loose and porous. It can be seen in the image magnified in 50 k times that the formation and growth of oxides on the surface of the film are highly disordered. The co-oxide crystals formed firstly in particles, and then grew in line and finally in the shape of pieces with a cross structure. No microbe can be found on the surface or in the cracks of the film. The quantitative analysis from EDS shows that the film consists of iron and manganese oxides.

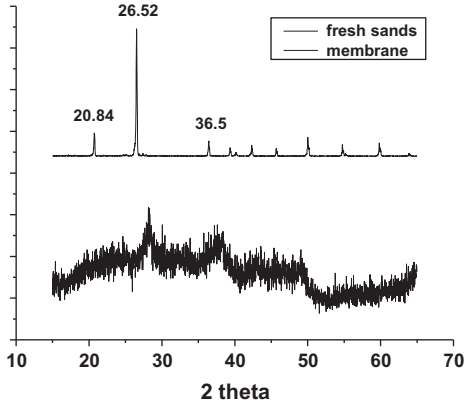

Fig. 4. The XRD pattern of fresh sands and co-oxide membrane.

Fig. 7(a) and (b) show that the physical structure of the co-oxide film was obviously damaged when treated at high temperature and pressure. The film was chapped and peeled partly from the surface of the sands. Compared with the surface of the film before treatment (Fig. 6(b)), the surface of the treated film rested on the sands (Fig. (7c)) was smoother and most of the tabular and threadlike oxide structures were not observed. The image amplified in 300 times shows that the film has a bilayer structure. The inner layer with a compact structure is nearly 5 μm thick and the outer layer with a loose structure is nearly 25 μm thick. After 178 h operation, the morphology of the treated film shown in Fig. 7(d) is the same as that of the film not treated (Fig. 6(c)), and also, no microbe was detected. So, related to the performance of the pilot-scale filter discussed before, one may come to a conclusion that the removal of ammonia in the filter is a catalytic oxidation process. The co-oxide film, which has catalytic activity on ammonia oxidation, was physically damaged by the treatment at high temperature and pressure and the removal of ammonia was decreased at the beginning of the operation. As the operation went on, the surface structure of the film was restored after 116 h and the capacity of the removal of ammonia got obviously recovered.

3.2.3. Specific surface area and pore properties

The specific surface area and pore size of the fresh sands and co-oxidize-coated film were measured by BET method. The results are shown in Table 3.

Compared with the fresh sands, the specific area of the film-coated sands was increased from 0.107 to $4.5\,m^2\,g^{-1}$, which was attributed to the formation of the porous film; the pore volume increased from 2.803×10^{-4} to $1.565 \times 10^{-2}\,cc\,g^{-1}$, and the average pore size increased from 10.5 to 13.91 nm, correspondingly. Since the specific area and the pore volume increased, more active sites were provided for the ammonia catalytic oxidation.

3.2.4. X-ray photoelectron spectroscopy

The chemsorption is the fundamental and previous step for catalytic reactions and so it is necessary to study the chemical adsorption sites of ammonia and dissolved oxygen in catalytic oxidation of ammonia happening on the surface of the film. The XPS spectra

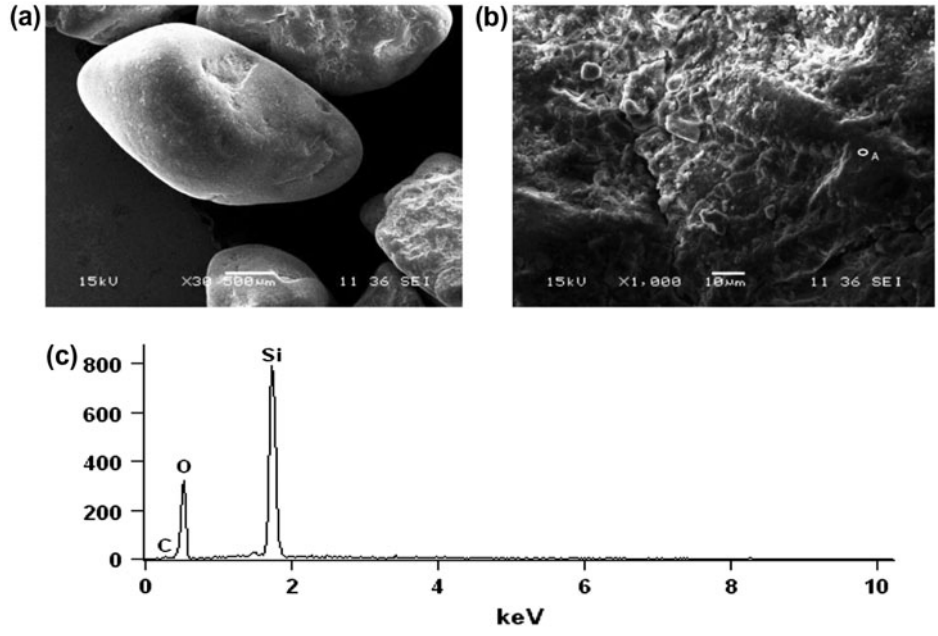

Fig. 5. SEM images of the fresh sands amplified in (a) 30 times; and (b) 1 k times. (c) EDS of the point A.

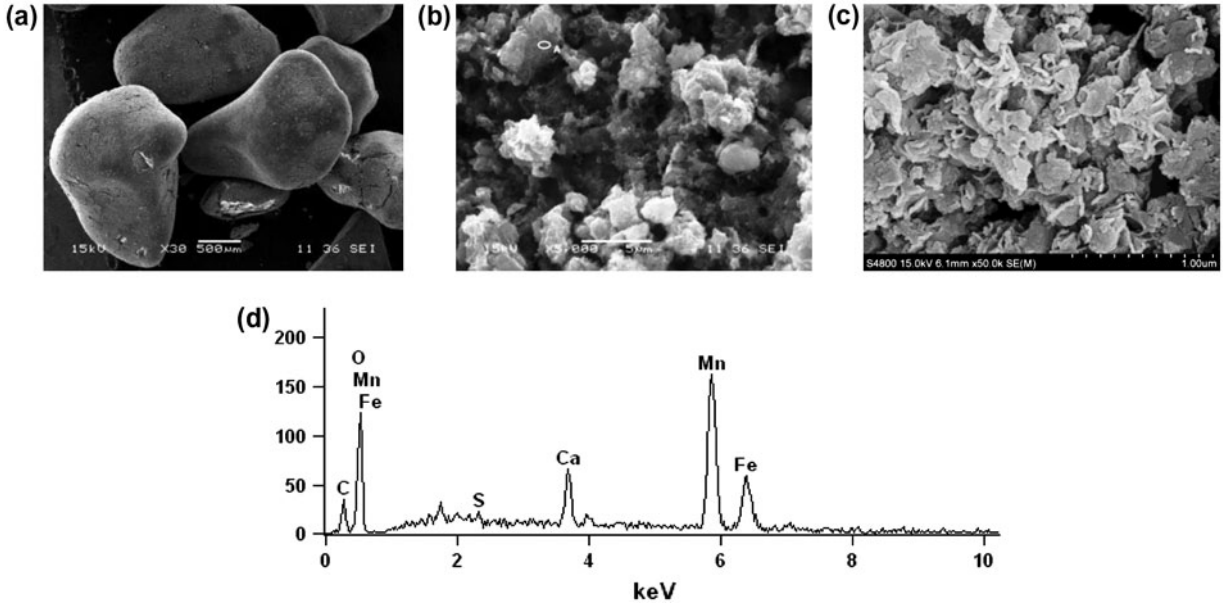

Fig. 6. SEM images of the co-oxide film-coated sands amplified in (a) 30 times; (b) 5 k times; and (c) 50 k times. (d) EDS of the point A.

of Mn3/2p and Fe3/2p of the film before and after the DO chemsorb equilibrium are shown in Fig. 8.

Fig. 8(a) shows the XPS data in Mn3/2p region before and after the adsorption of DO on the co-oxides film surface and obvious changes occurred. Since the electronegativity of Mn atoms in oxides is lower than O atoms, the growths of intensities and binding energies at 641.83 and 643.56 eV, at expenses of 641.51 and 642.97 eV before adsorption correspondingly, identify the formation of chemical bonds between O and Mn atoms. Being the chemisorb sites, Mn atoms occur as Mn_2O_3 at 641.51 eV [20] and as

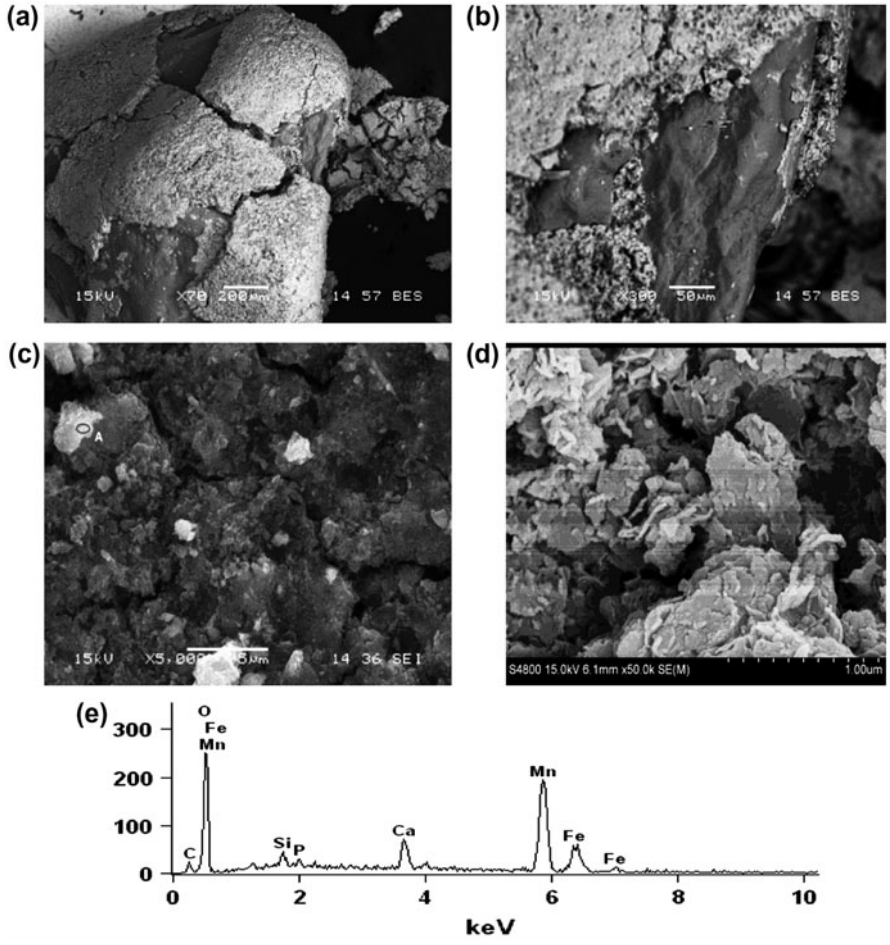

Fig. 7. SEM images of the treated co-oxide film-coated sands amplified in (a) 70 times and (b) 300 times; (c) the treated co-oxidize film-coated sands amplified in 5 k times; and (d) the treated co-oxidize film-coated sands after 178 h operation in 50 k times. (e) EDS of the point A.

Table 3
The specific surface area and pore properties of filter materials

Samples	Specific surface area, $m^2 g^{-1}$	Pore volume, $cc\,g^{-1}$	Average pore diameter, nm
Fresh sands	0.107	2.803×10^{-4}	10.5
Film-coated sands	4.500	1.565×10^{-2}	13.91

MnO_2 at 642.97 eV [21]. Similarly, Fig. 8(b) shows that in Fe3/2p region, the growth of binding energy at 709.63 eV, at expense of 709.11 eV before adsorption, identify the formation of chemical bonds between O and Fe atoms. Being the chemisorb sites, the Fe atoms occur as FeO at 709.11 eV [22]. The XPS spectra of O1s, Mn3/2p and Fe3/2p of film before and after the ammonia chemsorb equilibrium are shown in Fig. 9.

As shown in Fig. 9(a), the XPS data in O1s region changed obviously after the adsorption of ammonia happened. Three fitted peaks before the adsorption, 533.97, 532.07, and 530.20 eV, decreased to 532.46, 530.87, and 529.53 eV, respectively. This may be attributed to the bonding effects of N in ammonia to the atoms of Mn and Fe in oxides [23]. The generated N-Mn or N-Fe units may have reduced the outer electronegativity of the O atoms of oxides, and made the binding energies of O1s decreased. Fig. 9(b) shows the XPS data in Mn3/2p region before and after the adsorption of ammonia happened on the co-oxide film surface. It was found that the binding energy before

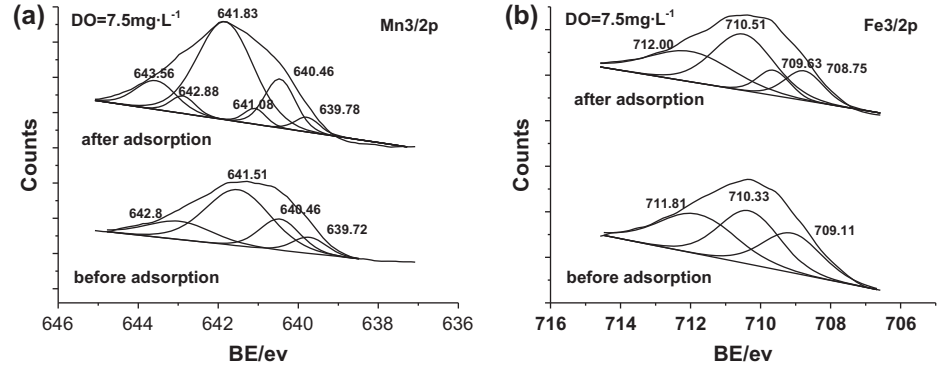

Fig. 8. The XPS spectra of (a) Mn3/2p and (b) Fe3/2p in film before and after the DO adsorption.

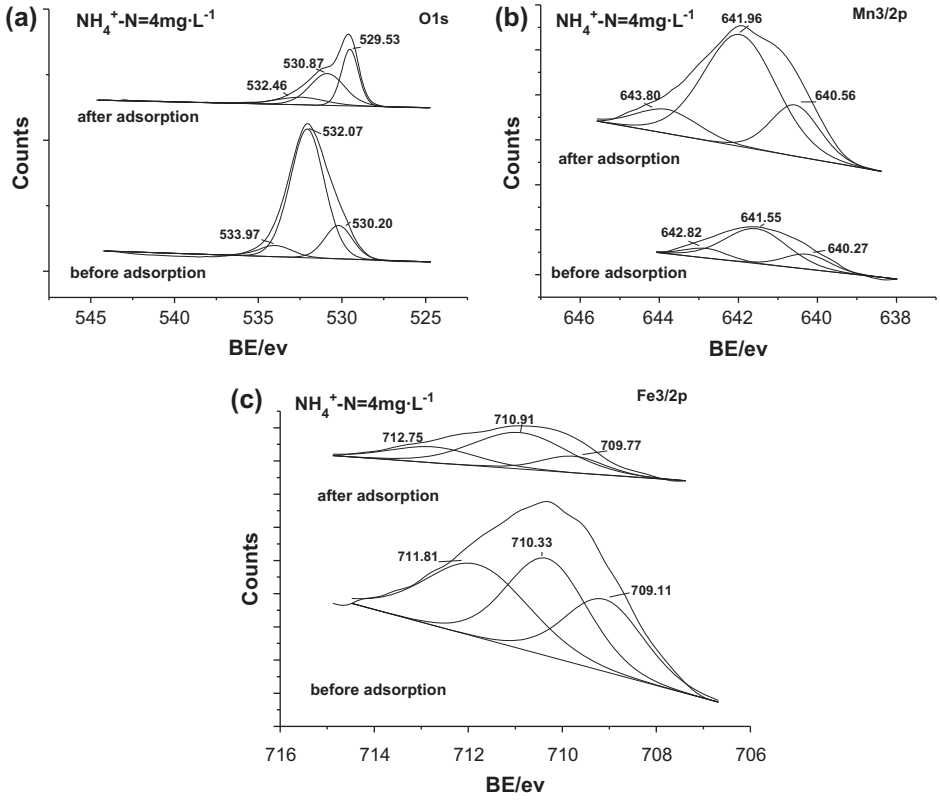

Fig. 9. The XPS spectra of (a) O1s, (b) Mn3/2p and (c) Fe3/2p in films before and after the ammonia adsorption.

the adsorption at 642.82, 641.55, and 640.27 eV increased to 643.80, 641.96, and 640.56 eV respectively. Since the electronegativity of Mn atoms in oxides is lower than that of N atoms in adsorbed ammonia, it is identified the changes in binding energies of Mn due to the chemical bonds of N-Mn formed in the adsorption process. The Mn atoms occurring as Mn_2O_3 at 642.82 and 641.55 eV [24] and MnO at 640.27 eV [20] are the chemisorb active sites of ammonia.

Fig. 9(c) shows that the XPS data in Fe3/2p region before and after the adsorption of ammonia happened on the co-oxide film surface. The binding energy before adsorption at 711.81, 710.33, and 709.11 eV increased to 712.75, 710.91 and 709.77 eV correspondingly. The binding energy increase identified that the chemical bonds of N and Fe were formed in the adsorption process, and the Fe atoms occurring as Fe_2O_3 at 711.81 [25] and FeO at 710.33 and 709.11 eV [26,27] are the chemisorb active sites of ammonia.

4. Conclusion

The Fe-Mn co-oxide film, formed on the sands surface in the filter process of high ammonia-, iron- and manganese-contained groundwater, gets amorphous structure, and increases the specific area and pore volume of the sands. The removal of ammonia recovered in 116 h after the coated sands got treated at high temperature and pressure, which was attributed to the restoration of the chemical and physical properties of the film surface. The amplified images of the film show that there is no microbe on the surface, and the chemical states of N transferred in the treatment indicated that the removal of ammonia is a catalytic oxidation process. The XPS characterization identified that the chemsorb active sites of dissolved oxygen are Mn atoms occuring as Mn_2O_3 and MnO_2, and the Fe atoms occuring as FeO, and that the chemsorb active sites of ammonia are the Mn atoms in states of Mn_2O_3 and MnO, and the Fe atoms in states of Fe_2O_3 and FeO.

Acknowledgement

This work was supported by the National Natural Science Foundation of China (Grant No. 51278409).

References

[1] N. Longo, M.F. Beal, J.B. Martin, Inherited disorders of amino acid metabolism in adults, In: A.S. Fauci, T.R. Harrison (Eds.), Harrison's Principles of Internal Medicine, vol. 364, McGraw-Hill, New York, NY, 1998, pp. 3214–3219.
[2] G.M. Enns, Neurologic damage and neurocognitive dysfunction in urea cycle disorders, Semin. Pediatr. Neurol. 15 (2008) 132–139.
[3] World Health Organization, Guidelines for Drinking Water Quality, WHO, Geneva, Switzerland, 2008.
[4] K.W. Tang, D.S. Zhu, Y. Tang, Y. Wang, Groundwater quality assessment of urban drinking water sources in China, Water Res. Prot. 25 (2009) 1–4.
[5] G. Moussavi, S. Talebi, M. Farrokhi, M. Farrokhi, R.M. Sabouti, The investigation of mechanism, kinetic and isotherm of ammonia and humic acid co-adsorption onto natural zeolite, Chem. Eng. J. 171 (2011) 1159–1169.
[6] M.Y. Li, X.Q. Zhu, F.H. Zhu, G. Ren, G. Cao, L. Song, Application of modified zeolite for ammonium removal from drinking water, Desalination 271 (2011) 295–300.
[7] A.G. Tekerlekopoulou, D.V. Vayenas, Ammonia, iron and manganese removal from potable water using trickling filters, Desalination 210 (2007) 225–235.
[8] E.M. Seeger, P. Kuschk, H. Fazekas, P. Grathwohl, M. Kaestner, Bioremediation of benzene-, MTBE-and ammonia-contaminated groundwater with pilot-scale constructed wetlands, Environ. Pollut. 159 (2011) 3769–3776.
[9] K.R. Zhu, H. Fu, J.H. Zhang, X.S. Lv, J. Tang, X.H. Xu, Studies on removal of NH_4^+-N from aqueous solution by using the activated carbons derived from rice husk, Biomass Bioenergy 43 (2012) 18–25.
[10] Y. Wang, Y. Kmiya, T. Okuhara, Removal of low-concentration ammonia in water by ion-exchange using Na-mordenite, Water Res. 41 (2007) 269–276.
[11] M. Li, C.P. Feng, Z.Y. Zhang, R. Zhao, X.H. Lei, R.Z. Chen, N. Sugiura, Application of an electrochemical-ion exchange reactor for ammonia removal, Electrochim. Acta 55 (2009) 159–164.
[12] A. Andersson, P. Laurent, A. Kihn, M. Prévost, P. Servais, Impact of temperature on nitrification in biological activated carbon (BAC) filters used for drinking water treatment, Water Res. 35 (2001) 2923–2934.
[13] H.A. Hasan, S.R.S. Abdullah, S.K. Kamarudin, N.T. Kofli, Response surface methodology for optimization of simultaneous COD, NH_4^+-N and Mn^{2+} removal from drinking water by biological aerated filter, Desalination 275 (2011) 50–61.
[14] I. Kasuga, H. Nakagaki, F. Kurisu, H. Furumai, Predominance of ammonia-oxidizing archaea on granular activated carbon used in a full-scale advanced drinking water treatment plant, Water Res. 44 (2010) 5039–5049.
[15] W.W.J.M. de Vet, R. Kleerebezem, P.W.J.J. van der Wielen, L.C. Rietveld, M.C.M. van Loosdrecht, Assessment of nitrification in groundwater filters for drinking water production by qPCR and activity measurement, Water Res. 45 (2011) 4008–4018.
[16] D.M. DeMarini, Genotoxicity of disinfection by-products: Comparison to carcinogenicity, Encycl. Environ. Health 2 (2011) 920–926.
[17] AWWA, American Public Health Association, Standard Methods for the Examination of Water and Wastewater, 19th ed., APHA, Washington, DC, 1995.
[18] T. Štembal, M. Markić, N. Ribičić, T. Štembal, F. Briški, L. Sipos, Removal of ammonia, iron and manganese from groundwaters of northern Croatia—pilot plant studies, Process Biochem. 40 (2005) 327–335.
[19] N.D. Kim, H.J. Yun, I. Nam, I.K. Song, J. Yi, Effect of thermal treatment on the structural characteristics and electrochemical properties of amorphous Mn oxide prepared by an ethanol-based precipitation method, Curr. Appl. Phys. 12 (2012) 1139–1143.
[20] B.N. Ivannov-Emin, N.A. Nevskaya, B.E. Zaitsev, T.M. Ivanova, Synthesis and properties of calcium and strontium hydroxomanganates (III), Russ. J. Inorg. Chem. 27 (1982) 1755–1757.
[21] R.O. Ansell, T. Dickinson, A.F. Povey, An X-ray photo-electron spectroscopic study of the films on colored stainless steel and colored "Nilomag" alloy 771, Corros. Sci. 18 (1978) 245–256.
[22] D.G. Zetaruk, N.S. McIntyre, X-ray photoelectron spectroscopic studies of iron oxides, Anal. Chem. 49 (1977) 1521–1529.
[23] G.D. Cui, C. Yang, G.Q. Gao, The surface morphology and structure of two-pole sputtered iron nitroen oxide thin films, J. Funct. Mater. 36 (2005) 783–785.
[24] Y. Umezawa, C.N. Reilley, Effect of argon ion bombardment on metal complexes and oxides studied by x-ray photoelectron spectroscopy, Anal. Chem. 50 (1978) 1290–1295.
[25] P. Mills, J.L. Sullivan, A study of the core level electrons in iron and its three oxides by means of X-ray photoelectron spectroscopy, J. Phys. D: Appl. Phys. 16 (1983) 723–732.
[26] G.C. Allen, M.T. Curtis, A.J. Hooper, P.M. Tucker, X-Ray photoelectron spectroscopy of iron–oxygen systems, Dalton Trans. 14 (1974) 1525–1530.
[27] D. Brion, Etude par spectroscopie de photoelectrons dela degradation supercielle de FeS_2, $CuFeS_2$, ZnS et PbS a láie et dans léau [Photoelectron spectroscopy study of the surface degradation of FeS_2, $CuFeS_2$, ZnS and PbS in air and in water], Appl. Surf. Sci. 5 (1980) 133–152.